Nuclear Instruments and Methods in Physics Research B 384 (2016) 30–36

Contents lists available at ScienceDirect

Nuclear Instruments and Methods in Physics Research B

journal homepage: www.elsevier.com/locate/nimb

Systematics of heavy-ion charge-exchange straggling

P. Sigmund [a,*], A. Schinner [b]

[a] Department of Physics, Chemistry and Pharmacy, University of Southern Denmark, DK-5230 Odense M, Denmark
[b] Department of Experimental Physics, Johannes Kepler University, A-4040 Linz, Austria

ARTICLE INFO

Article history:
Received 18 June 2016
Received in revised form 11 July 2016
Accepted 22 July 2016

Keywords:
Stopping power
Straggling
Swift heavy ions
Charge states
Shell effects

ABSTRACT

The dependence of heavy-ion charge-exchange straggling on the beam energy has been studied theoretically for several ion-target combinations. Our previous work addressed ions up to krypton, while the present study focuses on heavier ions, especially uranium. Particular attention has been paid to a multiple-peak structure which has been predicted theoretically in our previous work.

For high-Z_1 and high-Z_2 systems, exemplified by U in Au, we identify three maxima in the energy dependence of charge-exchange straggling, while the overall magnitude is comparable with that of collisional straggling. Conversely, for U in C, charge-exchange straggling dominates, but only two peaks lie in the energy range where we presently are able to produce credible predictions. For U–Al we find good agreement with experiment in the energy range around the high-energy maximum.

The position of the high-energy peak – which is related to processes in the projectile K shell – is found to scale as Z_1^2, in contrast to the semi-empirical $Z_1^{3/2}$ dependence proposed by Yang et al.

Measurements for heavy ions in heavy targets are suggested in order to reconcile a major discrepancy between the present calculations and the frequently-used formula by Yang et al.

1. Introduction

The phenomenon of charge-exchange straggling was predicted by Flamm and Schumann precisely 100 years ago [1]. In brief, a charged particle penetrating through matter may undergo a sequence of electron capture and loss processes while slowing down. Since the energy loss depends on the ion charge, capture and loss processes give rise to a fluctuation (straggling), in the energy loss. This 'charge-exchange straggling' adds to 'collisional straggling' [2], which also acts in the absence of charge exchange.

On the basis of a theoretical model involving two charge states [3] and a systematic study of hydrogen and helium ions in gas targets [4], the generally accepted view has become that charge-exchange straggling gives rise to a distinct maximum in the dependence of energy-loss straggling on the ion energy for ions with atomic number $Z_1 \geqslant 2$. This view has been strengthened by an analysis of experimental straggling data available in 1991 [5]. That analysis resulted in a frequently-used empirical formula that indicates a straggling peak at an energy $\propto Z_1^{3/2}$ with a peak height $\propto Z_1^{4/3}/Z_2^{1/3}$ relative to the Bohr formula for collisional straggling. Peak heights up to two orders of magnitude above Bohr straggling were predicted for very heavy ions. Experimental support for such pronounced effects came with measurements involving Pb and U ions [6] in the MeV/u energy range. For a recent summary the reader is referred to Ref. [7].

In a joint experimental and theoretical effort [8,9] on krypton and silicon ions in gas targets we confirmed the existence of pronounced maxima, up to two orders of magnitude above the Bohr value. In several cases we found reasonable agreement between experimental data and theoretical predictions, although pronounced discrepancies were found in others. In a parallel theoretical study [10] we predicted that at least two peaks must be found in the energy dependence of charge-exchange straggling. We also found that the leading (high-energy) peak is related to the charge equilibrium between the bare ion and a hydrogen-like ion.

The fact that the leading peak in charge-exchange straggling is related to processes in the K shell of the projectile has a number of implications. Firstly, its position in energy space must be expected to scale as $\propto Z_1^2$ rather than $Z_1^{3/2}$ as proposed in Ref. [5] or, as one might have expected from the Thomas–Fermi model, $\propto Z_1^{4/3}$. Secondly, secondary maxima as well as minima in straggling must be expected likewise to be related to the filling of projectile shells. We wish to address these questions in the present study and to identify ion-target combinations and energy regimes where these effects should be pronounced or, at least, visible in measurements.

The theoretical basis for our work in this area has been a general formalism [11], which expresses charge-exchange straggling by

* Corresponding author.
E-mail address: sigmund@sdu.dk (P. Sigmund).

http://dx.doi.org/10.1016/j.nimb.2016.07.016
0168-583X/

transition probabilities or cross sections for all relevant electronic transitions in the projectile. The formalism was first applied in a systematic study of the evolution of energy-loss spectra with the travelled pathlength ([12] and earlier work cited there). Subsequent work focused on straggling in charge equilibrium [13]. Making use of the smooth dependence of the mean energy loss on the ion charge we were able to express charge-exchange straggling by a simple relation involving the evolution of charge fractions with traveled pathlength and the variation of the stopping cross section with the ion charge.

Charge fractions as a function of travelled pathlength are the output of the ETACHA code [14] which, in principle, invokes all those cross sections that are needed in the computation of charge-exchange straggling. Extensive comparisons with experimental data have been performed by Imai et al. ([15] and earlier work cited there), showing qualitative agreement in the general trends.

We use ETACHA output as input into our calculation of charge-exchange straggling. In our previous work with this code [13,10] we had to cope with three limitations: Only ions up to Kr were allowed. The allowed energy range had a lower limit of 1 MeV/u, but the practical lower limit could actually be significantly higher. Moreover, numerical instabilities were frequently found. Specifically, the predicted equilibrium charge state was not always independent of the initial charge state. Since our routine involves small differences between large numbers, it is not easy to identify artifacts introduced by the numerical input.

A revised and expanded edition of the ETACHA code has appeared recently [16]. With an extension of allowed projectiles up to uranium we have now an opportunity to establish scaling relations in Z_1 and Z_2 for both peak position, height and width. At the same time, the relevant energy range expands, since the interesting upper energy limit increases $\propto Z_1^2$, while the lower limit does not. This is relevant for identifying more than one peak in the energy dependence of charge-exchange straggling.

When comparing with experimental straggling data we need to keep in mind that peaks are also present in the energy dependence of collisional straggling [17,18]. Such peaks appear near the stopping maximum and may increase straggling by up to a factor of three above the Bohr value [18]. They are caused by bunching of target electrons and increase in importance with increasing Z_2 where, conversely, charge-exchange straggling decreases in importance.

2. Recapitulation

We report computations on charge-exchange straggling by a procedure developed in Ref. [13] and applied to Kr and Si in gas targets in Refs. [8,10]. Here we briefly summarize the procedure.

The straggling parameter W is defined by

$$W(E,x) = \frac{d}{Ndx}\left\langle (\Delta E - \langle \Delta E\rangle)^2 \right\rangle, \tag{1}$$

where E denotes the beam energy, ΔE the energy loss of an ion after having traveled a pathlength x, N the number of target atoms per volume and $\langle \ldots \rangle$ an average over many trajectories.

Just as in the case of the mean energy loss, interest is primarily directed towards straggling in a charge-equilibrated beam. According to Refs. [11,13], straggling in charge equilibrium can be written in the form

$$W(E,\infty) \equiv W(E) = \sum_J F_J(E) W_J(E) + W_{\rm chex}(E), \tag{2}$$

where

$$W_{\rm chex} = 2N \sum_{JKL} F_J S_{JK} S_L \int_0^\infty dx\, [F_{KL}(x) - F_L], \tag{3}$$

and variables E have been suppressed for clarity. The quantity

$$S_{IJ} = \int T\, d\sigma_{IJ}(T) \tag{4}$$

denotes the stopping cross section for a collision with initial and final states I and J, respectively, and $d\sigma_{IJ}(T)$ the corresponding differential cross section. Moreover,

$$W_J \equiv \sum_L W_{JL}, \tag{5}$$

where

$$W_{JL} = \sum_L \int T^2\, d\sigma_{JL}(T) \tag{6}$$

is the corresponding straggling parameter. If the charge state is I at $x = 0$, $F_{IJ}(x)$ denotes the charge fraction of ions in state J after a path length x. The quantity $F_J \equiv F_J(\infty)$ represents the equilibrium charge fraction.

The first term on the right-hand side of Eq. (2) represents collisional straggling. Eqs. (4) and (5) indicate that energy loss in charge exchange, represented by terms for $I \neq J$, contributes to both collisional and charge-exchange straggling. In the following we consider only the charge-exchange term $W_{\rm chex}$.

A major simplification was found [13] by making use of the fact that the dependence of the stopping cross section $S_I = \sum_J S_{IJ}$ on the ion charge number q_J can be well approximated by a parabola over a generous interval. For diagonal elements, $I = J$, this assumption was based on calculations by our PASS code [19]. For off-diagonal terms an equivalent behavior was postulated, justified by the fact that energy loss by charge exchange is small compared to collisional energy loss for ions heavier than hydrogen. This point is discussed in appendix A.

For not too light ions, say, $Z_1 \gtrsim 10$, we found that between three neighboring charge states the above parabola can be well approximated by a straight line, so that

$$W_{\rm chex} \simeq 2N \left(\frac{dS}{dq}\right)_{q=\bar q(E)} \left(\frac{dS_{\rm coll}}{dq}\right)_{q=\bar q(E)} G_0(E), \tag{7}$$

where $S \equiv S(q)$ and $S_{\rm coll} \equiv S_{\rm coll}(q)$ represent the total frozen-charge stopping cross section and the collisional frozen-charge stopping cross section, respectively, $\bar q(E)$ is the mean equilibrium charge at energy E,

$$G_0(E) = \sum_J F_J(q_J - q)\beta_J, \tag{8}$$

and

$$\beta_J = \sum_L q_L \int_0^\infty dx (F_{JL} - F_L). \tag{9}$$

Inspection of Eq. (7) reveals that the effect of charge exchange on $W_{\rm chex}$ is contained in the factor $G_0(E)$, while the factors in front of $G_0(E)$ represent the variation of the stopping cross section with the ion charge. With this, the computational routine involves ETACHA for $G_0(E)$ and PASS for dS/dq.

Although the PASS code distinguishes between S and $S_{\rm coll}$, this distinction is hardly relevant within the overall accuracy of the theory which, as we shall see, is determined primarily by the ETACHA code. Therefore, following our previous procedure [13,10] we replace Eq. (7) by

$$W_{\rm chex} \simeq 2N \left(\frac{dS}{dq}\right)^2_{q=\bar q(E)} G_0(E), \tag{10}$$

in the following.

3. ETACHA calculations

3.1. The code

The revised ETACHA code comes in four versions, 23, 3, 34 and 4, which differ in the number of electrons and electron states involved. Versions 23 and 3 allow for three shells in the projectile ion, while versions 34 and 4 allow for four shells. This implies that at high beam energies, where only few projectile electrons are involved, we may expect Version 23 or 3 to be adequate, while decreasing beam energy requires to apply versions 34 or 4. In the examples presented in this work we apply versions 3 and 4 at high and low beam energies, respectively. Version 34 enters a single test run, while Version 23 – which is similar to the 1996 code [14] – has not been used here.

ETACHA output enters the computation of the quantity β_j in Eq. (9). As mentioned above, the computational routine built into ETACHA leads to occasional instabilities which may have a critical influence on our results. It is, therefore, essential to define a procedure on how to cope with such problems.

Fig. 1 shows two representative examples. The upper graph, 15 MeV/u iodine in carbon, shows the typical high-energy behavior with a reasonably well defined equilibrium charge state. Since a small difference remains at large depth, the integration has been limited by visual inspection to a depth at which equilibrium is apparently achieved. This truncation, indicated by a vertical line, is important to avoid a significant (depth-dependent) contribution from larger depths. Occasionally, discrepancies are found to increase with increasing depth. If a crossing point of all curves can be identified, the truncation line has been defined at that point.

The lower graph, 5 MeV iodine in carbon, shows a case where such a crossing point cannot be defined and where asymptotic equilibrium charges show a rather large spread. We have omitted such data in cases where neighboring energy values do not lead to such a behavior. In other cases this behavior indicates the lower energy limit for obtaining credible results.

The behavior of the two graphs in Fig. 1 is, qualitatively, typical for all ion-target combinations, although the observed artifacts may be both more or less pronounced. Moreover, the limiting energy between acceptable and unacceptable behavior varies between different ion-target combinations. A lower energy limit is found for all versions of ETACHA. This limit is lowest for ETACHA4, which allows for the largest number of electrons and states. The validity of all versions of ETACHA is currently limited to the nonrelativistic energy regime [16]. However, we also encountered another upper energy limit, above which ETACHA4 delivers unphysical results.

3.2. Straggling: influence of charge exchange

Fig. 2 shows $G_0(E)$ for U–Au and U–C over an energy range of up to three orders of magnitude. Here we focus on the qualitative information contained in these graphs, since quantitative predictions based on different versions of the ETACHA code show significant differences.

For U–Au there is a clear multiple-peak structure, although only ETACHA4 actually shows data points covering the third peak. For U–C, the lower energy limit where ETACHA3 delivers acceptable data, lies above the expected minimum. Here we rely on data from ETACHA4 which are more appropriate in the lower energy range.

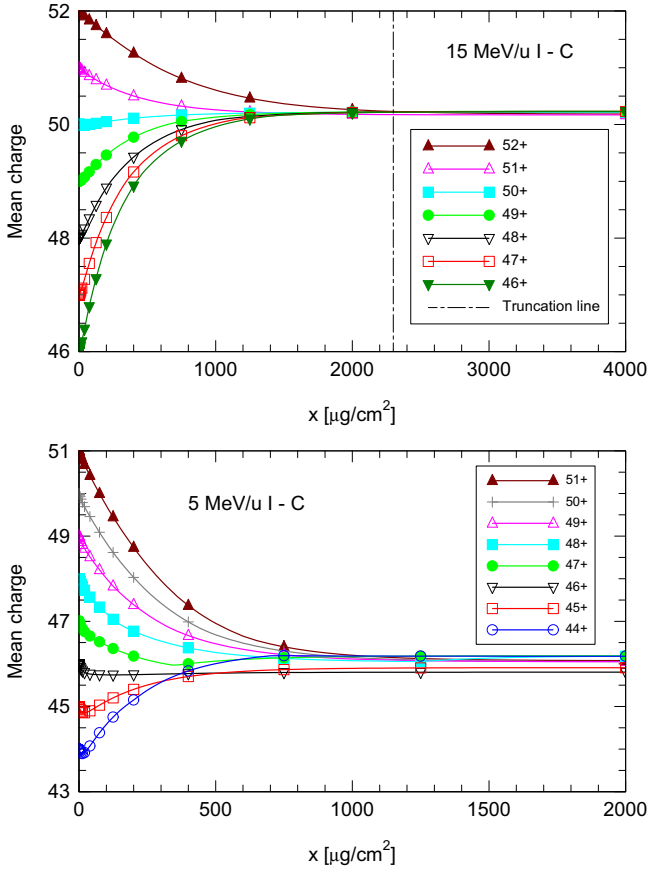

Fig. 1. Average charge state according to ETACHA3 for iodine in carbon versus travelled pathlength. Numbers indicate the initial charge state. Upper graph: $E = 15$ MeV/u; lower graph: $E = 5$ MeV/u.

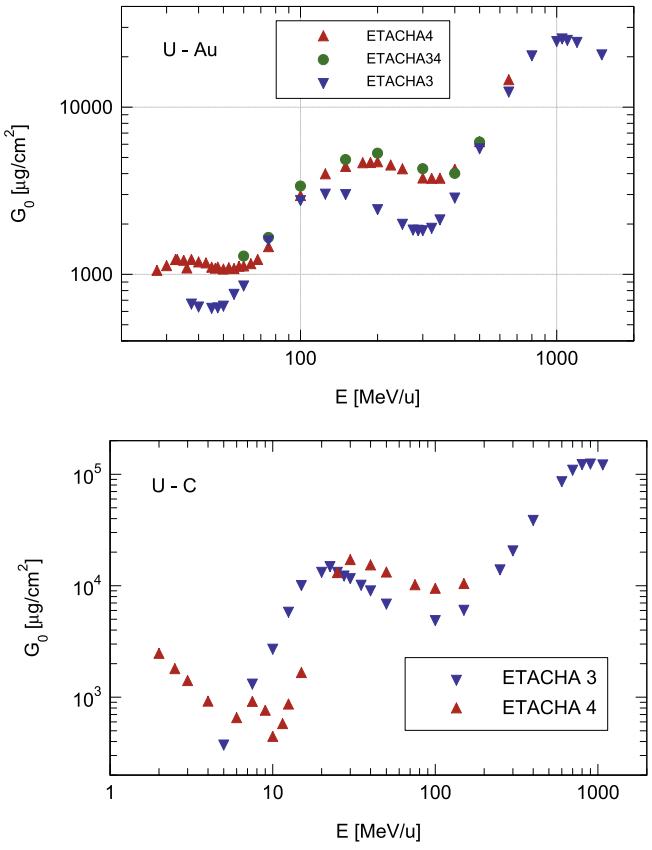

Fig. 2. The function $G_0(E)$ describing the effect of charge exchange on straggling in the U–Au (upper graph) and U–C (lower graph) system according to Eq. (7), evaluated from Eq. (8) with input from ETACHA3, 34 and 4.

In both cases the leading peak lies at $E \simeq 1000$ MeV/u. On the other hand, the distance between the first and the second peak is significantly wider in energy space for U–C than for U–Au. This confirms our previous experience [10,8] of a strong sensitivity of charge exchange on target properties that is absent in classical models [20,21].

However, significant differences are seen between the three versions in the position and magnitude of all but the leading maximum. This difference mainly reflects the number of electron states considered in the three versions. The good agreement between predictions of ETACHA34 and 4 from the first minimum downward in case of U–Au suggests that those results might be more realistic than those found from ETACHA3. Conversely, at higher energies, ETACHA3 and ETACHA4 yield almost identical results. Therefore there was no need to test ETACHA34 into that range.

3.3. Charge fractions

Fig. 3 shows the distribution of equilibrium charge fractions underlying the values of $G_0(E)$ in Fig. 2. In agreement with our conclusion in Ref. [10] we find that the leading maximum reflects the charge equilibrium between the bare ion and the one-electron ion.

The first minimum is found at an energy where the filled K shell is the dominating charge state. This reflects the stability of a closed K shell against electron capture and loss.

For the second maximum, ETACHA3 and ETACHA4 show shifted but otherwise rather similar distributions in case of U–Au, while there is good agreement for U–C. Both distributions are situated well inside the L shell.

These tendencies are less pronounced with regard to the second minimum and the third maximum. However, again the minimum shows a narrower distribution of charge fractions than the maximum.

Fig. 4 shows spectra for lighter ions, Kr–C and Ag–C, respectively, with very similar results.

3.4. Peak positions

One central result of Ref. [10] was that the leading peak in charge-exchange straggling was found close to the cross-over between the charge fractions of the bare ion and the one-electron ion. This implies that the leading peak is related to the K shell and, therefore, must follow a Z_1^2 dependence. The Bohr criterion [22] suggests that in charge equilibrium, electrons with orbital speeds exceeding the projectile speed v are bound to the projectile, while electrons with orbital speeds less than v are stripped. Thus, the leading peak in charge-exchange straggling should appear at a projectile speed where

$$v \simeq v_K = v_0 Z_1. \tag{11}$$

Fig. 5 shows peak positions calculated from Eq. (8) with input from ETACHA3 for a number of ions in carbon and gold. Our data for a carbon target show reasonable agreement with the scaling relation Eq. (11) for ions from helium to iodine, whereas significantly higher peak positions are predicted from gadolinium ions upward. Beam energies are here $\gtrsim 0.5$ GeV/u, where relativistic

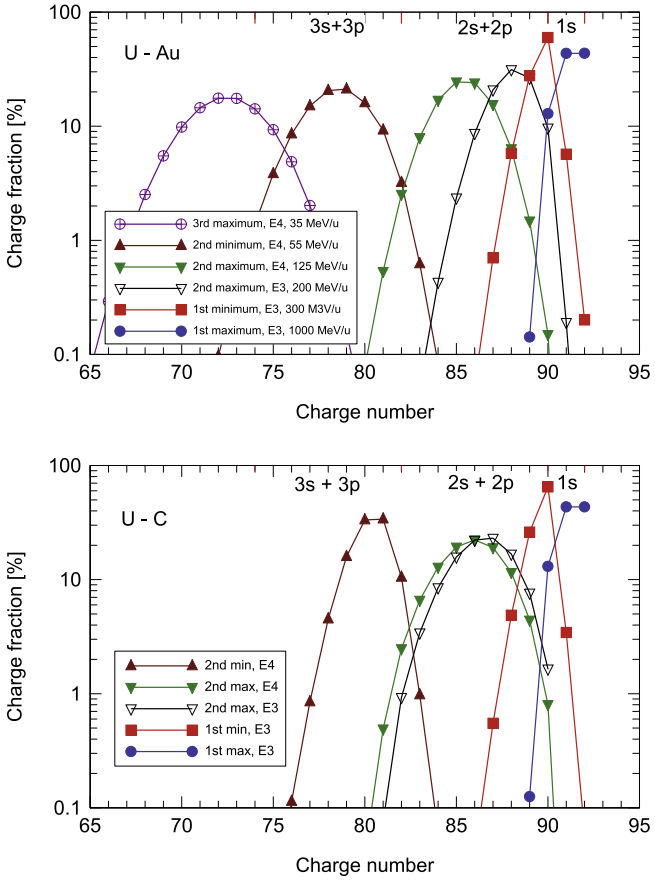

Fig. 3. Distribution of equilibrium charge fractions for U–Au (upper graph) and U–C (lower graph) at energies corresponding to maxima and minima of $G_0(E)$ shown in Fig. 2. E3 and E4 indicate the underlying ETACHA version. Red markers indicate boundaries in the projectile shell. Lines to guide the eye. (For interpretation of the references to color in this figure legend, the reader is referred to the web version of this article.)

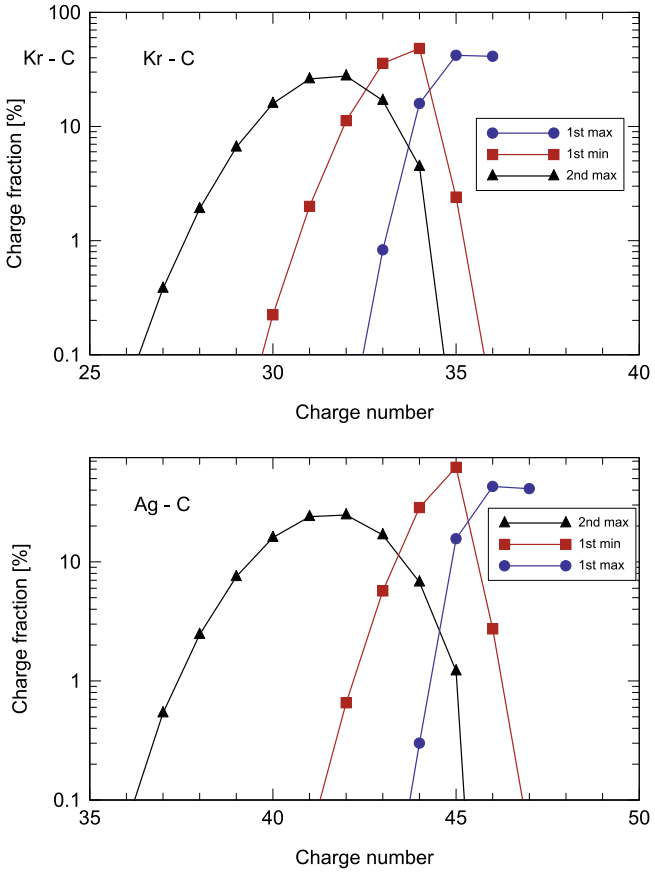

Fig. 4. Same as Fig. 3 for Kr- (top) and Ag–C (bottom). ETACHA3.

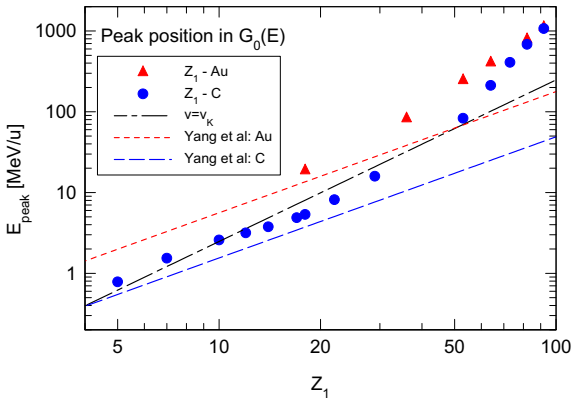

Fig. 5. Position of the leading peak in $G_0(E)$ versus the atomic number Z_1 of the ion. Triangles: calculated from ETACHA3 for gold target; circles: calculated from ETACHA3 for carbon targets. Dot-dashed line: Eq. (11); Dashed line: Peak in charge-exchange straggling predicted from Ref. [5] for carbon target; dotted line: from Ref. [5] for gold target.

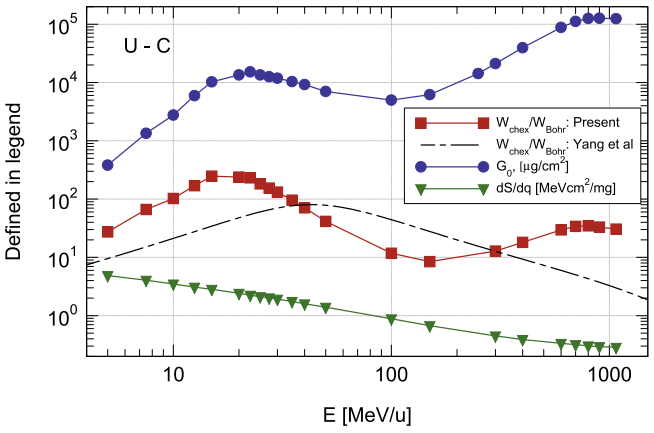

Fig. 6. Charge-exchange straggling of uranium ions in amorphous carbon. Evaluated from Eq. (7) on the basis of PASS and ETACHA3 input. The line $G_0(E)$ has been taken over from Fig. 2. Also included is the prediction of Ref. [5].

effects become significant. The scaling relation Eq. (11) also appears to be obeyed reasonably well for a gold target, albeit with a slightly different proportionality factor.

Also included are predictions of Ref. [5]. These are predictions for the peak in charge-exchange straggling, which lie below the peak in $G_0(E)$, since dS/dq decreases with increasing energy. As expected, the dependence on Z_1 is underestimated slightly, but the order of magnitude appears well represented by the Yang formula. A more quantitative comparison will be seen in Fig. 9.

4. PASS calculations

The PASS code represents an implementation [19] of binary stopping theory [23] which, in turn, represents an extension of Bohr stopping theory [24]. In brief, the theory incorporates projectile screening by bound electrons and a shell correction to account for orbital motion of target atoms. It also incorporates nonperturbative effects and, via an inverse-Bloch correction, a smooth transition from the Bohr to the Bethe regime of stopping. Numerous comparisons with experimental data have ensured competitive predictions of stopping cross sections [19,25].

4.1. Procedure

The PASS code in its present from delivers stopping cross sections as a function of energy and charge state for a given ion-target combination. The critical quantity entering Eq. (7) is the derivative of the stopping cross section with respect to the ion charge. In order to avoid numerical differentiation we substitute

$$\left(\frac{dS(q)}{dq}\right)_{q=\bar{q}} \to S(\bar{q}-1/2)-S(\bar{q}+1/2)\equiv -\Delta S. \qquad (12)$$

The equilibrium charge $\bar{q}$ is taken as the one determined by ETACHA for every single data point.

Especially for high $Z_1, \Delta S$ is a small difference between large numbers. Within the accuracy of the PASS code this does not constitute a significant source of error.

4.2. Carbon target

Fig. 6 shows charge-exchange straggling for U ions in amorphous C. It is seen that the double-peak structure found in Fig. 2 is retained. Although peak positions are close to those found for $G_0(E)$, peak heights differ substantially. Indeed, the second peak now becomes more pronounced due to multiplication with the quantity $(dS/dq)^2$, which decreases with increasing energy in the covered energy interval, as does $S(E)$ itself.

It is seen that the ratio $W_{\rm chex}/W_{\rm Bohr}$ between charge-exchange straggling and Bohr straggling is predicted to vary between ~ 10 and ~ 300.

Also included in the graph is the prediction of Ref. [5]. Application of that formula in this graph is far away from the range of experimental data available at the time of its inception. While it does not predict two peaks, the order of magnitude is compatible with our result.

4.3. Gold target

Fig. 7 shows equivalent results for U in Au. With regard to the difference between the results from ETACHA3 and ETACHA4 we refer to the comments made in relation to Fig. 2. While there appears strong evidence for the existence of three peaks, the overall magnitude of $W_{\rm chex}/W_{\rm Bohr}$ is significantly lower than in case of U–C. We have experienced this feature in our previous work [8] when studying straggling of krypton ions in gases from He to Kr. The origin of this decrease with increasing Z_2 is to be sought in the denominator, since Bohr straggling is proportional to Z_2 while charge-exchange straggling is not. This feature is absent in the formula from Ref. [5] which, consequently, predicts a value an order

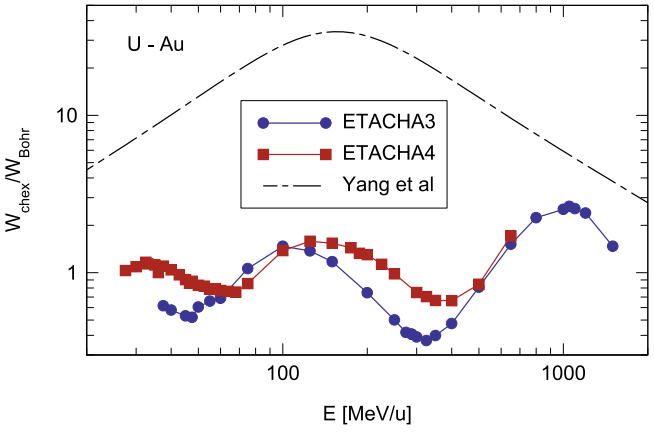

Fig. 7. Same as Fig. 6 for uranium ions in gold. Relative charge straggling only; predictions on the basis of ETACHA3 and ETACHA4 with Yang et al. [5].

of magnitude higher. Straggling measurements for heavy ions in heavy targets are of interest in this context.

4.4. Aluminium target

Fig. 8 shows equivalent results for U in Al, based on ETACHA3. Also included are experimental results for total straggling as well as results of a Monte Carlo simulation by Weick et al. [26]. While we find good agreement between theory and experiment, we emphasize that our calculation does not incorporate relativistic effects. The measurements cover the regime around the leading peak, and in agreement with the present finding the Monte Carlo simulations indicate a rapid decrease in straggling with decreasing energy. However, Monte Carlo calculations were not performed at lower energies and therefore did not catch the predicted minimum.

4.5. The first peak

Fig. 9 shows the variation of the position and height of the first peak in charge-exchange straggling, i.e. the peak at the highest energy, as a function of the atomic number of the ion. As expected, the peak height is an order of magnitude smaller in gold than in carbon. Compared with the Z_1 dependence of the peak position on energy, the variation of the peak height with energy is moderate.

Also included are predictions according to the formula of Yang et al. [5] which already were shown in Fig. 5, but now in the right context. Comparison with the predictions of the present work confirms the conclusions drawn from Fig. 5.

5. Conclusions

Considering the magnitude of differences between predictions based on different versions of the ETACHA code we focus on qualitative rather than quantitative conclusions. Within this margin, other sources of error such as ignoring the difference between total and collisional stopping cross sections, lack of relativistic corrections and approximations underlying Eq. (7), are of minor significance. Summing up we conclude that

- We have found three maxima in the energy dependence of charge-exchange straggling for U in Au. This feature is asserted to be typical for high-Z_1-high-Z_2 systems.
- The relative magnitude of these peaks compared to collisional straggling decreases with increasing Z_2. This is caused mainly by the Z_2 dependence of Bohr straggling.

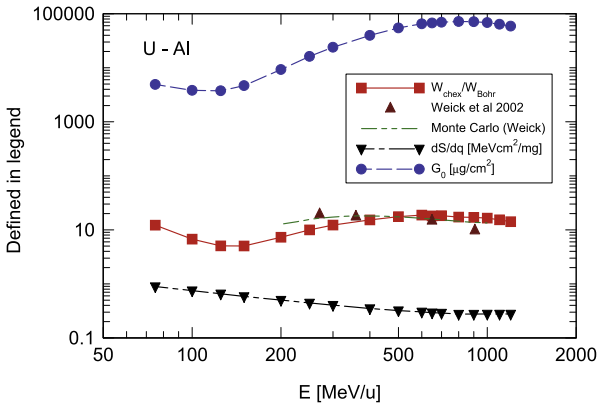

Fig. 8. Same as Fig. 6 for uranium ions in aluminium. Also included are experimental data and Monte-Carlo results from Weick et al. [26].

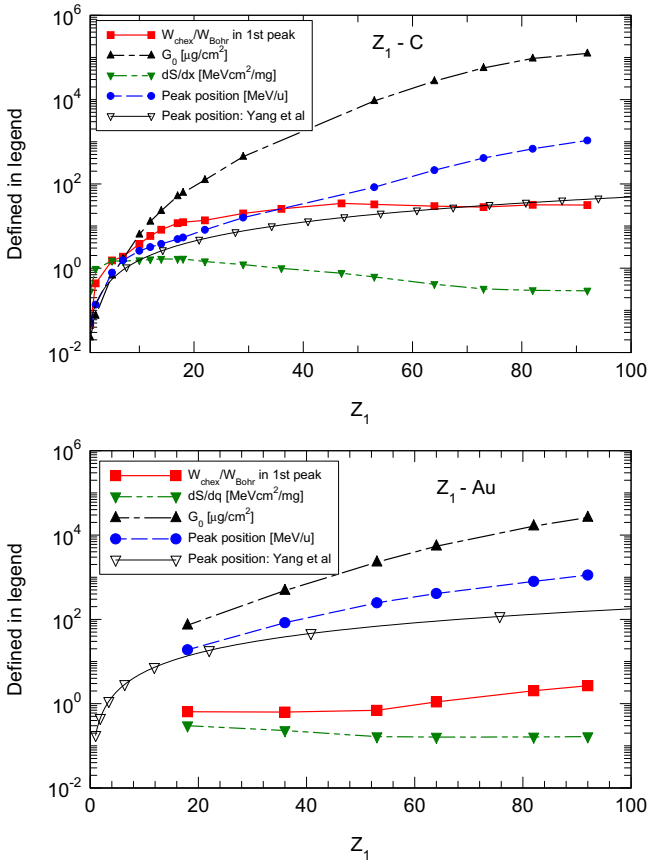

Fig. 9. Calculated Z_1 dependence of the height and position of the leading peak in straggling, compared with the position of the leading peak in $G_0(E)$ and dS/dq in charge equilibrium.

- The distance between peaks and their widths increases only slightly with increasing Z_2.
- For high-Z_1-low-Z_2 systems, exemplified by U in C, charge-exchange straggling dominates, but only two peaks have been found in the energy range where we were able to extract results from ETACHA.
- For U–Al our results agree with experimental results of Weick et al.
- The Z_1^2 dependence of the high-energy peak confirms that this peak reflects the filling of the K shell and differs from the $Z_1^{3/2}$ dependence suggested by Yang et al.
- Measurements of straggling for high-Z_1 ions in intermediate- and high-Z_2 targets are highly desirable.

Acknowledgement

This project has received continuous interest and stimulation from our experimentalist colleagues in Jyväskylä, Linköping, Zurich and La Chaux-de-Fonds. We wish to sincerely thank professors J. P. Rozet and D. Vernhet for making their new revised ETACHA codes available to us. Special thanks are due to our referee for pointing out a significant error in the first version of this paper. This work has been supported by the Carlsberg Foundation.

Appendix A. Role of energy loss in charge exchange

For a two-state system, statistical theory of charge-exchange straggling [11] predicts the following straggling formula,

$$W = \frac{1}{\sigma}(\sigma_{21}W_1 + \sigma_{12}W_2) + \frac{2}{\sigma^3}(S_1 - S_2)[(\sigma_{21}S_{11} + \sigma_{12}S_{21})\sigma_{12} - (\sigma_{21}S_{12} + \sigma_{12}S_{22})\sigma_{21}], \tag{13}$$

where σ_{12} and σ_{21} are the cross sections for charge exchange between two states 1 and 2, and

$$\sigma = \sigma_{12} + \sigma_{21} \tag{14}$$

the cross section for one charge-exchange cycle. Moreover, $S_{IJ} = \int T d\sigma_{IJ}(T)$ is the stopping cross section for a collision with initial and final state I and J, and

$$S_J = S_{J1} + S_{J2} \tag{15}$$

the stopping cross section for an ion in charge state J. Finally $W_{IJ} = \int T^2 d\sigma_{IJ}(T)$ is the straggling parameter and $W_J = W_{J1} + W_{J2}$.

Eq. (13) represents a convenient separation between collisional and charge-exchange straggling. Note, however, that this definition incorporates part of the energy loss in charge exchange in collisional straggling.

With the replacements $S_{11} = S_1 - S_{12}$ and $S_{22} = S_2 - S_{21}$ we can write Eq. (13) in the form

$$W = \frac{1}{\sigma}(\sigma_{21}W_1 + \sigma_{12}W_2) + \frac{2\sigma_{12}\sigma_{21}}{\sigma^3}(S_1 - S_2)^2 + \frac{2}{\sigma^2}(S_1 - S_2)(\sigma_{12}S_{21} - \sigma_{21}S_{12}) \tag{16}$$

Finally, expressing

$$S_{12} = T_{12}\sigma_{12}; \qquad S_{21} = T_{21}\sigma_{21}, \tag{17}$$

where T_{12} is the average energy transfer in a charge-exchange event from state 1 to 2, we find

$$W = \frac{1}{\sigma}(\sigma_{21}W_1 + \sigma_{12}W_2) + \frac{2\sigma_{12}\sigma_{21}}{\sigma^3}(S_1 - S_2)[(S_1 - S_2) + \sigma(T_{21} - T_{12})]. \tag{18}$$

If the term $\sigma(T_{21} - T_{12})$ in the square brackets is neglected, Eq. (18) reduces to the standard expression [3] with the important addition that all energy loss incorporates energy loss in charge exchange. Whether or not this is an adequate approximation depends on whether

$$\sigma|T_{21} - T_{12}| \ll |S_1 - S_2|. \tag{19}$$

As an example, consider 700 MeV/u U in Al, where

$$\begin{aligned} \sigma_{1s} &= 0.0368 \times 10^{-20}\ \text{cm}^2; \\ \Delta T \simeq m v^2/2 &= 0.384\ \text{MeV}; \\ \sigma\Delta T &\simeq 0.141 \times 10^{-15}\ \text{eVcm}^2; \\ \Delta S &= 12 \times 10^{-15}\ \text{eVcm}^2, \end{aligned}$$

so that neglecting the perturbing term causes an error of $\sim 1\%$ in this case.

References

[1] L. Flamm, R. Schumann, Ann. Phys. 50 (1916) 655.
[2] N. Bohr, Philos. Mag. 30 (1915) 581.
[3] B. Efken, D. Hahn, D. Hilscher, G. Wüstefeld, Nucl. Instrum. Methods 129 (1975) 219.
[4] F. Besenbacher, J.U. Andersen, E. Bonderup, Nucl. Instrum. Methods 168 (1980) 1.
[5] Q. Yang, D.J. O'Connor, Z. Wang, Nucl. Instrum. Methods B 61 (1991) 149.
[6] H. Weick, H. Geissel, C. Scheidenberger, F. Attallah, T. Baumann, D. Cortina, M. Hausmann, B. Lommel, G. Münzenberg, N. Nankov, F. Nickel, T. Radon, H. Schatz, K. Schmidt, J. Stadlmann, K. Sümmerer, M. Winkler, H. Wollnik, Nucl. Instrum. Methods B 164–165 (2000) 168.
[7] P. Sigmund, Particle Penetration and Radiation Effects Volume 2, 179 Springer Series in Solid State Sciences, Springer, Heidelberg, 2014.
[8] C. Vockenhuber, J. Jensen, J. Julin, H. Kettunen, M. Laitinen, M. Rossi, T. Sajavaara, O. Osmani, A. Schinner, P. Sigmund, H.J. Whitlow, Eur. Phys. J. D 67 (2013) 145.
[9] Vockenhuber, C., Thöni, M., Jensen, J., Arstila, K., Julin, J., Kettunen, H., Laitinen, M., Rossi, M., Sajavaara, T., Whitlow, H.J., Osmani, O., Schinner, A., Sigmund, P., 2014. Presented at ICACS 26 in Debrecen.
[10] P. Sigmund, O. Osmani, A. Schinner, Nucl. Instrum. Methods B 338 (2014) 101.
[11] P. Sigmund, Nucl. Instrum. Methods B 69 (1992) 113.
[12] L. Glazov, P. Sigmund, Nucl. Instrum. Methods B 170 (2000) 39.
[13] P. Sigmund, O. Osmani, A. Schinner, Nucl. Instrum. Methods B 269 (2011) 804.
[14] J.P. Rozet, C. Stephan, D. Vernhet, Nucl. Instrum. Methods B 107 (1996) 67.
[15] M.. Imai, M.. Sataka, M.. Matsuda, S.. Okayasu, K.. Kawatsura, K.. Takahiro, K.. Komaki, H.. Shibata, K.. Nishio, Nucl. Instrum. Methods B 354 (2015) 172.
[16] E. Lamour, P.D. Fainstein, M. Galassi, C. Prigent, C.A. Ramirez, R.D. Rivarola, J.-P. Rozet, M. Trassinelli, D. Vernhet, Phys. Rev. A 92 (2015) 042703.
[17] P. Sigmund, A. Schinner, Eur. Phys. J. D 23 (2003) 201.
[18] P. Sigmund, A. Schinner, Eur. Phys. J. D 58 (2010) 105.
[19] P. Sigmund, A. Schinner, Nucl. Instrum. Methods B 195 (2002) 64.
[20] N. Bohr, Phys. Rev. 58 (1940) 654.
[21] W.E. Lamb, Phys. Rev. 58 (1940) 696.
[22] N. Bohr, Mat. Fys. Medd. Dan. Vid. Selsk. 18 no. 8 (1948) 1.
[23] P. Sigmund, A. Schinner, Eur. Phys. J. D 12 (2000) 425.
[24] N. Bohr, Philos. Mag. 25 (1913) 10.
[25] ICRU, Stopping of ions heavier than helium, ICRU Report, vol. 73, Oxford University Press, Oxford, 2005.
[26] H. Weick, A.H. Sorensen, H. Geissel, C. Scheidenberger, F. Attallah, V. Chichkine, S. Elisseev, M. Hausmann, H. Irnich, Y. Litvinov, B. Lommel, M. Maier, M. Matos, G. Munzenberg, N. Nankov, F. Nickel, W. Schwab, T. Stohlker, K. Summerer, B. Voss, Nucl. Instrum. Methods B 193 (2002) 1.